DESIGN AND DEVELOPMENT OF THE EARTHCARE BROADBAND RADIOMETER MECHANISM ASSEMBLY

G Munro[(1)], M Hampson[(1)], M Humphries[(2)], S. Lewis[(1)]

[(1)]ESTL, ESR Technology Ltd, Whittle House, 410 The Quadrant, Birchwood Park, Warrington, WA3 6FW, UK
Email:grant.munro@esrtechnology.com
[(2)]SpaceMech Ltd, 36 Charlton Gardens, Westbury-on-Trym, Bristol, BS10 6LX

ABSTRACT

The Broadband Radiometer instrument is one of four instruments to fly on the EarthCARE spacecraft. The instrument will measure the top of atmosphere radiative flux to aid studies into the interactions between clouds, aerosols and radiation. At the heart of this instrument is a mechanism assembly, comprising two nested bearing assemblies driving a chopper drum and a calibration drum. The former controls the passage of light into the three telescopes while the latter positions the viewing baffles and calibration sources which are intermittently brought into view to calibrate the instrument. This paper presents an overview of the design and a description of the test program to date, including lessons learned during this time.

1. INTRODUCTION

The Broadband Radiometer instrument is one of four instruments to fly on the EarthCARE spacecraft, the third of ESA's Earth Explorer Core Missions. The mission aims to study the interactions between clouds, aerosols and radiation with the aim of improving future meteorological and climate models. The instrument will measure the top of atmosphere radiative flux at higher spatial resolutions than on previous instruments, confirming estimates derived from the cloud and aerosol profiles measured by the other instruments on the satellite [1].

At the heart of this instrument is a mechanism assembly (Fig 1), comprising two nested bearing assemblies driving a chopper drum and a calibration drum. The former controls the passage of light into the three telescopes while the latter positions the viewing baffles and calibration sources, which are intermittently brought into view to calibrate the instrument. Although both consist simplistically of a brushless DC motor and optical encoder, both have very different operational requirements in terms of load, lifetime and motion profiles.

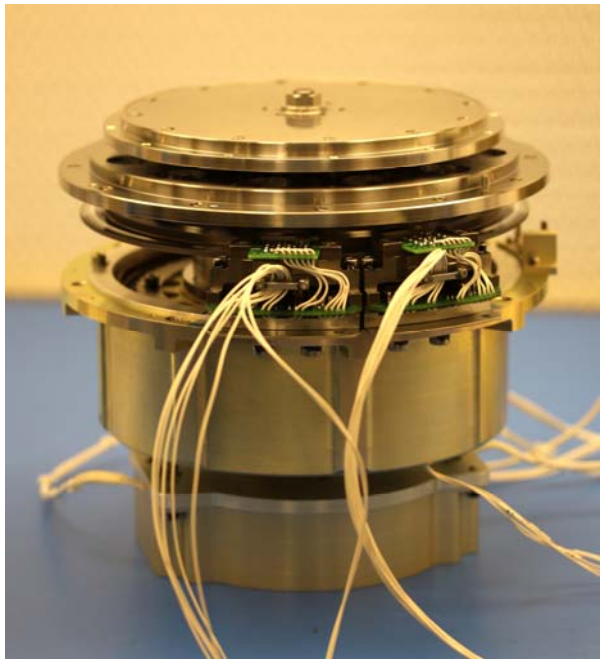

Figure 1. Mechanism Assembly – Radiator Removed

The testing of this mechanism reflects the proto-flight program chosen for the instrument as a whole. Within the program a total of five models are to be built as follows:

- 2 x Elegant Breadboard
- Life-test Model
- Proto-Flight Model
- Flight Spare

2. MECHANISM DESCRIPTION AND REQUIREMENTS

2.1. Overview of Main Requirements

The mechanism assembly consists of two main mechanism subsystems as well as including elements of the thermal control system. The assembly includes a common support structure around which the Calibration Target Mechanism (CTM) rotates, while the Chopper Drum Mechanism (CDM) shaft lies at the

'14th European Space Mechanisms & Tribology Symposium – ESMATS 2011'
Constance, Germany, 28–30 September 2011

centre. The outer housing forms the main interface to the instrument, where it is situated on the side wall of the aluminium honeycomb structure. There are also interfaces to both of the drums which are supplied as part of the Telescope Assembly, and both contain optical elements. A section view showing the main elements of the mechanism is shown in Fig 2.

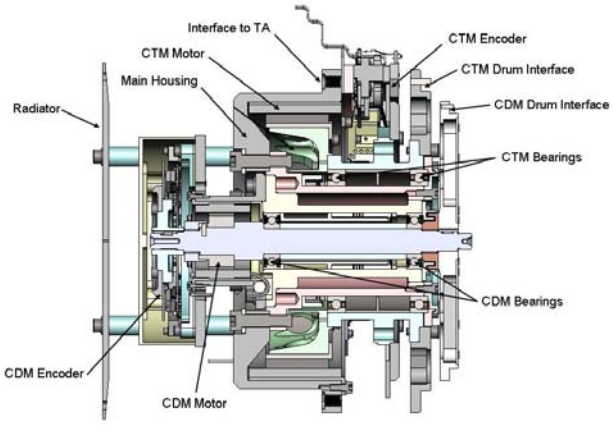

Figure 2. Mechanism Assembly Section

The mission lifetime is just under 37 months which equates to approximately 423 million revolutions of the chopper drum and just over 1 million calibration cycles on the Calibration Target Mechanism.

The instrument thermal environment is tightly controlled and the mechanism is designed to run between –35 and +30 degrees Celsius. The instrument thermal control system extends to the mechanism which includes a radiator with thermal tiles, monitoring thermistors and heaters.

The EarthCARE spacecraft carries additional payloads, some of which are sensitive to micro-vibrations. As such the exported forces and torques are assessed for each mechanism and there are requirements on balance grade and angular accelerations on each mechanism.

There are also extended requirements relating to contamination control, particularly because of the potential for laser induced contamination due to the presence of the LIDAR instrument ATLID.

2.2. Chopper Drum Mechanism

The chopper drum mechanism (CDM), at the centre of the assembly, rotates continuously at 261 rpm. This allows light to pass into the three telescope assemblies which gather measurement data in three viewing directions – fore, nadir and aft. Over the 3 year mission life-time this equates to just over 400 million revolutions. The mechanism employs PGM lubricated radial bearings with a low preload appropriate to the lubricant. These are also sputtered with MoS_2 on the raceways to provide further lubrication.

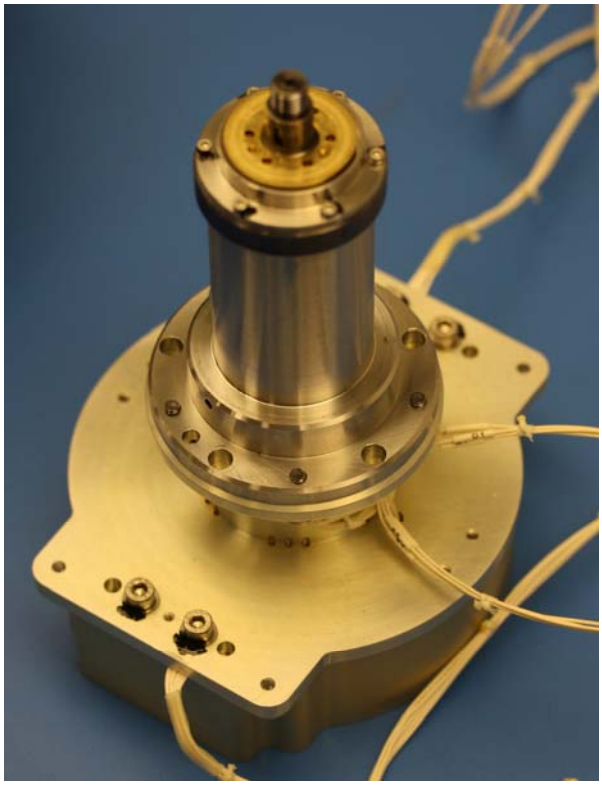

Figure 3. Chopper Drum Mechanism

PGM was chosen following a trade-off of the candidate lubricants. The main advantages include:

- Ability to accelerate life-test
- Heritage in long life applications in bearings of this size
- No viscous losses due to the presence of oil – particularly at low temperatures.
- Cleanliness
- Available as standard items from bearing suppliers

Since this lubricant has a critical Hertzian contact stress limit of 1200MPa, the preload was set to a low enough level to ensure a long life [2][3]. In this case 20N is applied, which equates to a maximum contact stress of 890 MPa. Since the chopper drum has no other conductive path to ground, the bearings must also be able to dissipate any charge from the drum. Despite the semi-conducting properties of the MoS_2, it has been shown that the bearings can dissipate sufficient charge to function as the sole conductive path for this purpose .

The bearings themselves are SR8 deep groove radial bearings, which have optimised conformity to increase the axial load capacity. As is normal in radial bearings the axial load is limited by the truncation, or overriding, of the lands rather than the raceway contact

stress. These are used in angular contact mode in a back to back configuration, preloaded by a customised spring and snubber arrangement designed to limit the axial displacement of the shaft. This is primarily to protect the encoders and quartz filters on the drum and the snubber stiffness is controlled to minimise shocks transmitted through to these components.

The mechanism employs a direct drive system using a zero-cogging brushless DC motor with redundant windings sourced from Aeroflex. This offers a simple and reliable architecture with minimum mass and cost. The absence of any contacting elements ensures long life while the synchronous drive and zero-cogging design of the motor gives speed stability well within the ±0.25% requirement. The two phase motor is driven with a pulse width modulated drive using sine and cosine drive waveforms.

Finally, the mechanism uses optical encoders offering dual read heads for redundancy. This type of encoder has good flight heritage while it can also be customised to use high reliability components appropriate to the radiation environment. However, the chosen manufacturer, Gurley Precision Instruments in the USA, are new to the space industry and the encoders undergo a full qualification program prior to delivery. In the case of the CDM the encoder has 11 bit resolution, which gives 13 bits after quadrature. This encoder is situated within a housing at the rear of the CDM mechanism with the read-heads located on opposing sides of the disk.

2.3. Calibration Target Mechanism

The calibration drum mechanism (CTM) rotates a drum containing a number of viewing baffles, 4 black-body calibration sources, two black-body electronics assemblies, a fold mirror for the visible calibration assembly and a cassette of monitor photodiodes to measure the relative ageing of the mirrors. This drum is required to perform regular periodic slews to bring the various calibration sources into view. Over the duration of the mission this mechanism will be required to perform just over 1 million high speed slews over ±25 º and 180º, the vast majority being over the smaller range. These slews are performed for total-wave (TW) calibration and short-wave (SW) calibration respectively. Magnetic detents are employed in the calibration locations and a magnetic end-stop is employed to act as a passive launch lock and optically-safe park position.

This larger mechanism uses angular contact bearings lubricated using physical vapour deposited (PVD) lead supplemented by a lead bronze cage. These are 71811 angular contact bearings from SKF-SNFA, which are equivalent to the former SEA55 bearing from SNFA. Once again the solid lubricant is compatible with accelerated testing, however the intermittent operation of this mechanism allows acceleration of the test purely by reducing the time between slews. The high contact stress capability of the lead lubricant is also appropriate because of the larger CTM rotating mass, which requires a higher preload of 1 000N. The use of sputtered lead in the range 0.2 – 0.5µm has significant heritage for bearings of this size, which have been used in a number of successful missions. In particular the Giotto de-spin mechanism and the AMSU-B scanner used identical bearing and lubricant combinations, the latter having achieved operational success on three separate missions with a more highly dynamic scan profile than required for this mechanism.

As for the CDM mechanism a two phase direct drive brushless DC motor is used. This mechanism periodically rotates the calibration sources into the telescope field of view approximately every 90 seconds, before returning to its nominal earth view position. This mechanism is driven according to predefined profile drive tables, consisting of position and feed-forward values, and also employs a 400Hz PID (proportional integral derivative) control loop to correct for any position errors relative to this profile.

The CTM encoder is similar in design to the smaller CDM encoder although this has a higher resolution of 12 bits, giving 14 bits after quadrature. This encoder is not housed and the read-heads are located adjacent to each other, either side of the nominal imaging position.

The CTM mechanism has a number of magnetic detents built into its function, including a magnetic launch park detent and end-stop. This also includes redundant micro-switches, which are activated by a cam on the rotating structure, and indicate when the mechanism is in the park position. These features are critical to ensure that the optical path remains light tight during launch and early spacecraft operations, ensuring that the sensitive detectors are not unintentionally exposed to damaging sunlight.

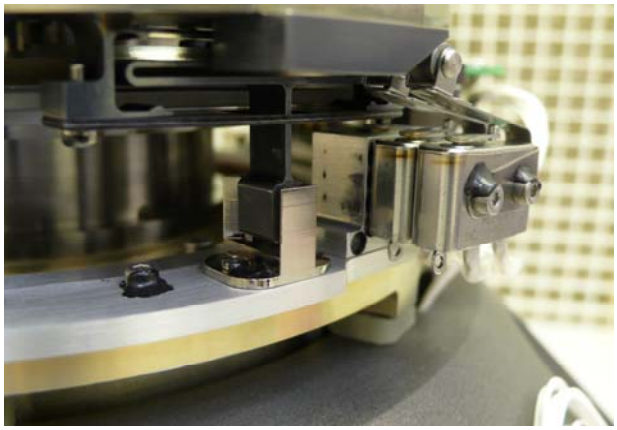

Figure 4. Flexible Magnet Arm in Detent Position

A compliant flexible arm is used in combination with the end-stop to which minimises disturbances to the

spacecraft and ensures that the restoring function of the magnet is maximised (Fig. 4). It also helps to minimise the contact force with the end-stop enhancing the life of the MoS_2 lubrication at the contact and reducing the risk of fretting.

The compliance of the end-stop is particularly important during switch on or recovery from any anomaly where the ICU loses the encoder position. In this case the drum can be driven to the safe park position under hardware control. However the stepping nature of this motion results in potentially damaging impacts or bouncing against the end-stop. This compliance minimises any problems during this basic form of operation, which is sensitive to motor pole alignment, by ensuring that the drum will be captured and retained by the magnets.

2.4. Common Design Features

Features common to both bearing systems include a spring and snubber arrangement tailored to each mechanism. This consists of a controlled compliance spring element and a displacement limiting snubber tube which sits within or around it, as shown for the CTM mechanism in Fig 5. In both mechanisms this is used to limit the displacement of the shaft in the direction of the spring. This ensures that the spring element can be compliant enough to ensure good torque stability under varying thermal gradients, while the snubber prevents excessive motion of the shaft under externally applied loading. In both cases the tightly set gap between the encoder disk and reticle is in the non-sprung direction of the bearing system to ensure that this gap is maintained. However the snubber ensures that excessive displacements are not observed when the load is transmitted through this spring, although it has a controlled compliance to minimise any shock loading caused by this contact.

Figure 5. CTM Spring and Snubber Arrangement (section and full view)

This arrangement ensures that there is enough compliance to ensure that the preload can be set correctly and that it is relatively insensitive to thermal gradients or settling, while at the same time limiting the gapping and shock loading associated with excessively rigid snubbers. For the CDM bearings, which can only be used for long life applications with a low level of preload, this arrangement is particularly useful in controlling the overall load-deflection characteristics.

Another common feature of the mechanisms is the presence of a purge path for use during ground testing. This ensures that the on-ground life is maximised for the purposes of verifying the function of the instrument. Since MoS_2 in particular is damaged by excessive running in air, the N_2 environment allows the amount of ground running to be increased to more practical durations. The benefits also extend to the lead lubricated bearings, particularly when being run in the horizontal axis, since the on-ground flight-like performance is prolonged in this unfavourable orientation. This purging system allows the bearing cavities to be continuously purged with nitrogen during ground running, with labyrinth seals maintaining a small positive pressure within the cavity. For the avoidance of contamination, these seals are also present to ensure that the dominant venting path is away from the optical elements of the Telescope Assembly. The vent paths are also completely independent to ensure that there is no cross contamination between the two lubrication systems.

3. QUALIFICATION AND LIFE-TESTING

At the time of writing the life-test is entering the orbital simulation phase of the test program, having completed the on-ground allocation and a pre-conditioning vibration test in which it experiences qualification levels. The experience gained from the breadboard models and the high level of representivity of the life-test model ensures that the mechanism performance is already well known before commencing the build of the flight models.

3.1. Life-test Programme

The life-test has been designed to closely match the intended verification activities at all stages of the instrument and spacecraft AIV programme. As such usage requirements based on environment and orientation of the mechanism are defined, and the life-test includes phases appropriate to combinations of these two parameters. The life test is conducted with mass representative dummy drums and the flex-harness which allows power and signal transfer to and from the calibration drum electronics in place. The set-up is shown in Fig. 6.

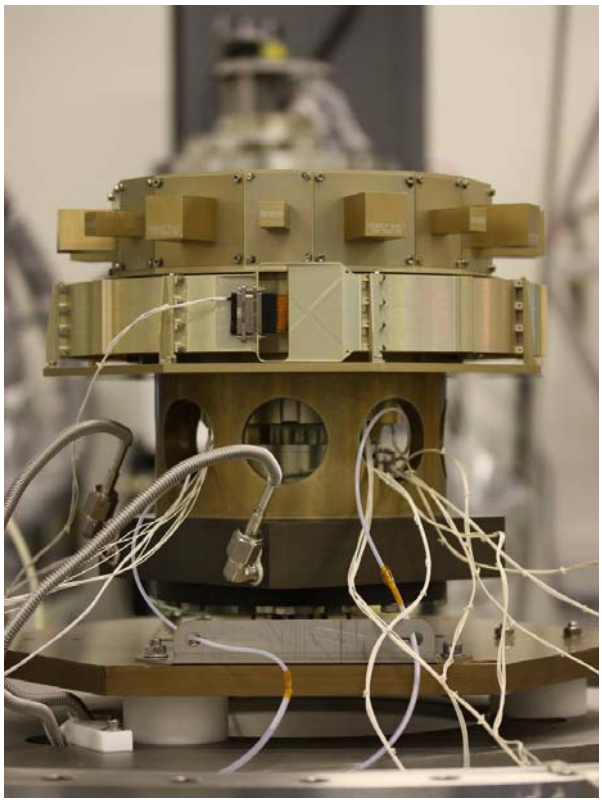

Figure 6. Life-test – Vertical Configuration

For the purposes of applying margin to the ground testing durations the margin is applied according to ECSS-E-ST-33-01 to the sum of these ground test cycles. An overall factor is then applied to each phase such that the additional cycles are distributed proportionally between the different phases. Since the two mechanisms are considered separately these margins are applied to each separately. In addition the two different slew types on the CTM are also treated individually. This is a more conservative application of the margins for the CTM, although the number of short-wave calibration slews, over 180º, is relatively small and so it does not significantly affect the overall number of cycles, or the time taken to complete the test.

The use of solid lubricants allows the acceleration of the life-test and so testing in vacuum was conducted at a rate up to 10x the nominal speed of 261 rpm, although trials were performed to identify any cage stability problems prior to running at high speed. Any speeds at which the torque noise became disproportionally high would be avoided due to the likely increased wear between the bearing and the dynamically unstable cage.

The vibration test is conducted with the primary aim of pre-conditioning the bearings prior to the orbital phase of the life-test. According to ECSS standards this should envelope the cumulative total of vibration tests at all levels, while also including one-time exposure to qualification levels for the qualification duration. Since the PFM programme includes an element of qualification vibration for the flight mechanism, this was applied concurrently with this requirement such that the durations at qualification level do not represent a significant over-test of the mechanism. At the time of writing this test has just been successfully completed.

The final orbital phase of the life-test is then run in vacuum for the duration of the orbital cycles. So that this phase most accurately reflects the zero-g orbital environment the mechanism is oriented vertically and the chopper drum is removed to minimise the net axial load on the bearing system. Since the mechanism runs at a constant speed this reduction of the inertia is not deemed to be significant in terms of the life-test. In terms of the removal of any imbalance forces, this was found to be insignificant compared to the additional contact stress as a result of the drum mass. The proposed configuration is therefore the most representative. The initial part of this life-test incorporates the thermal vacuum testing, while the remaining cycles are subjected to further longer term thermal variations within the expected operational limits. This ensures some degree of representivity with respect to the orbital environment and prevents the bearings from running over too narrow a running track.

The overall programme is being run according to the duration shown in Tab. 1.

Table 1. Life-test Durations

	Environment	CDM Factored	TW Factored	SW Factored
Life-test Part A	Vertical / N2	9,391,020	38,730	39
	Vertical / Vac	33,883,401	139,741	142
	Horizontal / N2	1,319,363	5,441	6
	Horizontal / Vac	558,841	2,305	2
	Total Ground	45,152,625	186,217	189
Life-test Part B	Vertical / Vac	528,602,060	1,427,060	2,280
	Total	573,754,685	1,613,277	2,469

3.2. Functional Testing

The performance of the bearings is confirmed by periodic functional tests. Since the mechanism is being self-driven this is the only time it is possible to measure some of the performance indicators. These functional tests include measurement of the CDM bearing torque by performing a coast down test and special constant speed test slews on the CDM through the full angular range. The torque data is obtained from the facility monitoring software while the power and speed/position data are obtained from the mechanism life-test controller telemetry files.

CDM functional tests (Fig. 7) consist of a run up to the nominal 261rpm operating speed, a period of stabilisation at this speed then an unpowered coast down to rest. Speed stability and power dissipation are measured over the latter part of the constant speed part of the profile, while the mean bearing torque is measured at the end of the coast down.

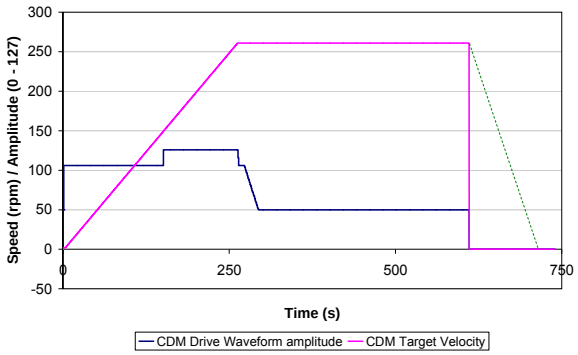

Figure 7. CDM Functional Test

The CTM functional test (Fig. 8) consists of a test slew profile to give an indication of the power dissipated in the mechanism. To ensure a complete sweep of the CTM mechanism range, a constant speed test slew was included to enable a torque estimation based on drive power dissipation to be carried out.

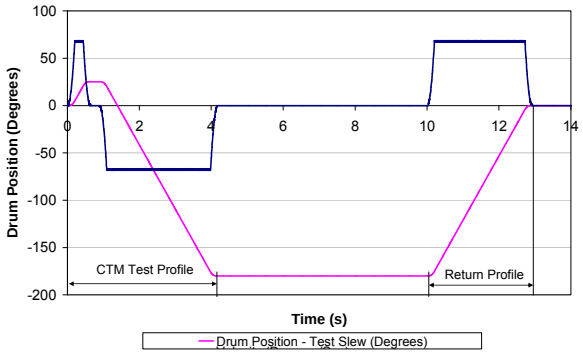

Figure 8 CTM Functional Test

The test consists of a constant velocity sweep from the total-wave detent adjacent to the end stop to the short-wave detent, the two angular extremes of the operational profiles. In should be noted that, because the drum is self driven and there are still relatively high accelerations, the torque observed during this test is the reaction torque of the accelerating drum inertia and not a direct measurement of bearing torque. This can only be estimated by looking at the power dissipation during the constant speed portion of the slew. Since the magnitude of the torque variations experienced as the flex-arm passes through the detents is constant, this power fluctuation can be scaled to give the overall relationship between power and torque. This does however require the drum to be externally driven to be able to characterise these torque variations.

A final test combines the CDM and CTM running and verifies that these run as expected concurrently, while giving an indication of the combined performance of the mechanism. This data provides complete torque data for comparison with the exported torque requirements.

3.3. Performance Indications

Following completion of the ground phase of the life test, a good estimation of the overall performance can be made. In addition to the functional tests performed as part of the life-test, other characterisation checks had already been carried out which confirm the basic performance of the motors and bearings.

During Part A of the life-test the varying test environments and orientations gave some variations in performance, not unexpected for the configuration and lubricants (Fig 9). For the CDM mechanism these variations were apparent during transitions from one environment to another, where the lubricant was essentially being run in each time. During both vacuum phases the torques stabilised to nominal levels after a few hundred thousand revolutions. The horizontal running however produced higher torques than anticipated. Although these do not pose a problem to testing due to the relatively large motor margins, they give an indication of non-ideal cage behaviour. In general it was also found that the overall torques were slightly higher than anticipated, which can be attributed to additional magnetic losses as the result of the proximity of local magnetic steel structure surrounding the bearings. Since the preload is relatively low, this additional torque as well as the latent torque of the motor was a significant contributor to the overall mean torque.

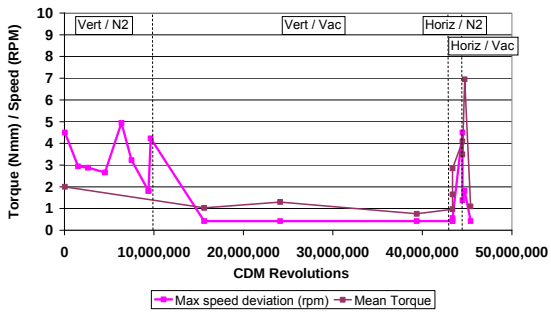

Figure 9. CDM Torque and Speed Data

Although it is not a functional requirement of the mechanism to perform at accelerated speeds, some useful lessons were learned from the accelerated running in vacuum. Perhaps counter-intuitively, the lower torque performance of the MoS_2 bearings in vacuum was most likely to experience problems with motor synchronisation. The reduction in stability caused by the reduced friction, combined with the reduction in motor torque at higher speed meant that it became difficult to accelerate the mechanism to the full intended 10x acceleration for the vacuum phases of the test. Rather than spend a significant amount of time trying to optimise the acceleration profile of the drum and increasing the period resolution of the drive tables, it was decided, for these relatively short phases, to run at a slightly lower speed up of to 8x acceleration.

The functional testing of the mechanism gave positive results with the synchronous motor giving good speed stability. Despite a relatively long period for which it took any speed disturbances from the acceleration profile to decay, the speed settled to well within the ±0.25% requirement (equivalent to 0.65rpm) and close to the resolution limit of the speed sensing.

The CTM also showed significant variations between the different environments (Fig 10). In particular the higher friction and adverse gravity vector in the horizontal orientation under N_2 purge gave significantly higher torques. Despite a cage design which aims to minimise the sensitivity to this type of cage misbehaviour, the power dissipation over the full range of the short-wave calibration slew progressively increased with the number SW cycles. This is symptomatic of blocking behaviour in bearings oscillating over relatively large angles and is caused by lateral creepage of balls with respect to the running track. This then leads to increasing ball-cage interactions which become progressively worse [4]. Fortunately this 'blocking' misbehaviour takes many more cycles to build up than are required for ground testing and it is therefore not expected to pose any risk to proper function during ground testing. There is also no evidence that this will be evident during the low-friction, zero-g, orbital environment, which is closest to the stable vertical vacuum phase, although this will be monitored closely during the rest of the life-test.

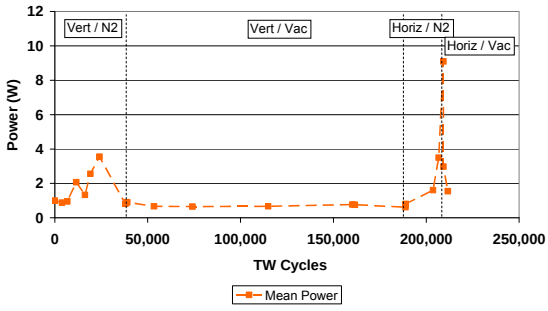

Figure 10. CTM Power Dissipation

Manual torque tests were used to support the power data taken from the motor telemetry and these showed the mechanism torque performance to be in line with predictions, with clear measureable torque variations due to the detents and micro-switch cam. The torque trace in Fig 11 shows a full rotation from the park position to the extreme end stop and back (the return rotation was performed faster, hence the shorter duration). The four detents can clearly be seen and also the torque due to the cam as the drum returns to its original park position. The highest torques are observed at each end stop as the drum is brought to rest, although these are not significant.

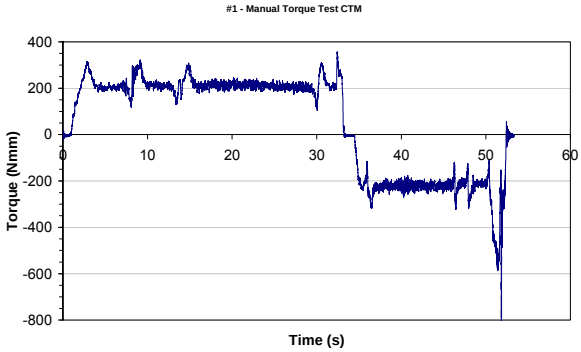

Figure 11. CTM Torque Profile

Despite efforts to eliminate any torsional dynamic modes of the test rig within the existing chamber during the design and early commissioning of the rig, the residual resonance at around 140Hz proved to be problematic, with significant torque noise associated with this mode. This represents a whole chamber resonance and so it is therefore difficult to remove easily without performing a significant modification to the facility. Because of the narrow frequency range of the associated resonances it is likely that a notch filter will be applied to the 400Hz torque data to eliminate this significant disturbance in future. This also ensures that no other higher frequency data is lost, although the most significant torque noise is otherwise in the sub 100Hz range. For such a sensitive test, with bearing torques on the CDM around 1Nmm, it is also important to eliminate any sources of vibration such as cryo-pumps as these may be very large in comparison to the measured torques for these lightly preloaded bearings.

4. LESSONS LEARNED

As for any mechanism project, a number of lessons were learned or re-learned during the development and testing of this mechanism assembly. Some important lessons are described here.

A number of lessons were learned relating to torque budgets for this programme. Firstly it is important to recognise all of the torque contributions in each mechanism, particularly where the bearing torques are low. Additional magnetic losses due to interactions between the motor magnets and any surrounding magnetically permeable material may contribute further residual torques to the mechanism and also affect the torque capability of the motor.

For synchronous motors the torsional stiffness of the drive may also give dynamic responses which demand greater than predicted torque from the motor in order to prevent loss of synchronisation. This may be hard to predict and assess in terms of motor margin, but it may be that lower bearing torques give the worst case motor margin. For the more complex closed loop CTM

control system it is also evi dent that there are difficulties relating to variations in frictional torque. For a mechanism which is ex pected to function in a number of orientations and environments, it is unlikely that optimum performance can be achieved by a single set of control parameters in all of these.

Despite efforts to eliminate rig resonances, sensitive tests such as these m ay be affected by modes of t he entire chamber or other modes that are increasi ngly hard to eliminate. These may well be significant, but if well characterised can be filtered out during post-processing. F requency domain analysis of torque data is critical an d effective in identifying torques relating to real mechanism and cham ber resonance contributions.

The implementation of t he high compliance magnetic end-stop was highly effective in restraining the CTM drum against rotation. This performed well despite the significant out of balance on the CTM mass dummy drum.

The high level of representivity of t he Life-test model has been critical in gaining a ful l understanding of mechanism performance. The self-driven nature of the test means that it is more difficult to obtain some of the normal torque data relating to bearing friction, but the representivity of the mechanism and the overall system performance in a wider context is m uch better understood.

Finally, as has been observed many times in the past, we have a m echanical system designed for a st ringent on-orbit requirement for which the exhaustive on-ground testing in adve rse spacecraft orientations represent considerable design challenges. Th is is almost beyond the c hallenge of achieving the performance required in zero-g vacuum.

5. CONCLUSIONS

The Broadband Radiometer instrument Mechanism Assembly is currently entering the long orbital simulation phase of the life-test, h aving completed the ground simulation life-test phase and a pre - conditioning vibration test in which it experience qualification levels. Th e manufacture of the flight models will commence shortly.

Performance appears close to that which was predicted for on orbit function, but the wide range of test configurations means that some reduction in performance may b e present during ground testing. These have been identified due to the highly representative life-test from which clear usage budgets for higher level testing can be derived.

The novel additions to this mechanism such as th e flexible magnetic end-stop and the preload spring and snubber arrangement have been demonstrated to be effective in their application.

6. ACKNOWLEDGEMENTS

The authors would like to acknowledge the support of our industrial partners on the BroadBand Radiometer Instrument: Systems Engineering a nd Assessment (SEA) Ltd and the R utherford Appleton Laboratory (STFC). We also gratefully acknowledge the support of Astrium and ESA for their guidance and thorough reviews during the development of t he instrument and mechanisms.

7. REFERENCES

1. Wallace K. et al. (2009), The BroadBand Radiometer on the EarthCARE Spacecraft, *Proc. SPIE Vol 7453*.
2. Anderson M.J. (1999), Further Tribological and Ball Bearing Tests to Evaluate Duroid Replacements, *Proc. 8th European Space Mechanisms & Tribology Symposium*, Toulouse.
3. Anderson M.J. (2001), Ball Bearing Tests to Evaluate Duroid Replacements, *Proc. European Space Mechanisms & Tribology Symposium*, Liege.
4. Roberts E.W. (1997), *Space Tribology Handbook, 4th Ed.*